Interrelation between Molecular Motions and Phase Transitions in Monomethylammonium Perchlorate. A Study by DSC, Proton, and Deuteron NMR

S. Jurga* and H. W. Spiess

Institute of Physical Chemistry, University of Mainz and
Max-Planck-Institut für Polymerforschung, Mainz

Z. Naturforsch. **40a,** 602–610 (1985); received April 4, 1985

Dedicated to Professor R. Kosfeld on the Occasion of his 60th Birthday

Differential scanning calorimetry, the temperature dependence of proton and deuteron lineshapes and spin-lattice relaxation times are reported for the isotopic species $CH_3NH_3ClO_4$, $CD_3NH_3ClO_4$ and $CH_3ND_3ClO_4$ of monomethylammonium perchlorate. The data confirmed the existence of three different phase modifications in monomethylammonium perchlorate and its selectively deuterated analogues. In addition they were used to identify the molecular motions occurring in the respective phases and to determine their activation parameters. In the low temperature phase III, stable below 320 K, the CH_3 and NH_3 groups reorient about their threefold symmetry axes C_3 with different frequencies. In the low-temperature range of this phase the deuteron quadrupole coupling constant indicates N–H ... O hydrogen bonds between the monomethylammonium and the perchlorate ions. In the intermediate phase II, between 320 K and 451 K for $CH_3NH_3ClO_4$ and $CD_3NH_3ClO_4$ and 320 K and 437 K for $CH_3ND_3ClO_4$, the methylammonium ions reorient about an axis inclined at an angle of 18 degrees to the C_3 axis. The analysis of the entropy changes, associated with the III–II transitions indicates that the ClO_4^- ions have a large motional freedom in phase II, presumably because of breaking or weakening of N–H ... O hydrogen bonds. In phase I the monomethylammonium ions undergo isotropic motion along with translational diffusion between different sites of the primitive cubic unit cell.

1. Introduction

In order to describe the physical state of solids which undergo polymorphic phase transitions, determination of the enthalpy changes associated with the transitions and the molecular motions in different phase modifications is of particular interest [1]. Differential scanning calorimetry (DSC) allows to determine the precise transition temperatures and the corresponding enthalpy changes. Nuclear magnetic resonance (NMR) in turn, especially if performed for different nuclei experiencing various types of nuclear interactions, provides unique information on the type and the time-scale of molecular motions [2]. It is the aim of this paper to report on DSC, proton and deuteron NMR studies of monomethylammonium perchlorate $CH_3NH_3ClO_4$ (1 MAP), and its selectively deuterated analogues $CH_3ND_3ClO_4$ (1 MA-dP) and $CD_3NH_3ClO_4$ (1 M-dAP). Solid 1 MAP exhibits, as shown by DTA and high-temperature x-ray techniques [3, 4] three different phase modifications. Since the monomethylammonium ion along with the anion of tetrahedral symmetry may be capable of orientational disorder the question arises, whether a given transition is induced by a correlated motion of both ions or whether it takes place due to a change of the motional behaviour of only one of the two ions. NMR studies allow to identify the motion of cations in the different phases and to determine their activation parameters. In addition they throw some light on hydrogen bonds N–H...O and the dynamics of the ClO_4-groups by analysing the deuteron quadrupole coupling constant and the entropy changes associated with the observed transitions. The results can be compared with those for trimethylammonium- and dimethylammonium perchlorates [5, 6] which also show three different phase modifications being achieved by a change in motional behaviour of both cations and anions. These NMR and DSC observations will provide a general picture of the interrelation between solid-solid phase transitions and molecular motions in multimethylammonium perchlorates. The low-temperature phase of $CH_3NH_3ClO_4$, below 321 K,

---

* Alexander von Humboldt fellow on leave from A. Mickiewicz University, Poznan, Poland.

Reprint requests to Prof. H. W. Spiess, Institut für Physikalische Chemie, Universität Mainz und MPI für Polymerforschung, Postfach 3148, D-6500 Mainz.

0340-4811 / 85 / 0600-0602 $ 01.30/0. – Please order a reprint rather than making your own copy.

crystallizes in the space group $P2_1/n$ with $Z = 8$, $a = 1.059$, $b = 0.767$ and $c = 1.287$ nm, and $\beta = 101°.26'$ [4]. The intermediate phase II, between 321 and 415 K, crystallizes in a tetragonal structure with $Z = 1$, $a = 0.387$ and $c = 0.929$ nm [3]. The high-temperature phase I, between 451 K and the melting temperature at 528 K, is of cubic primitive structure with $Z = 1$ and $a = 0.518$ nm [3]. The precise crystal structure information of phases II and I is not, however, available. Our preliminary studies of proton NMR linewidth and T_1 relaxation in $CH_3NH_3ClO_4$ [7] have shown that: (a) the CH_3 and NH_3 groups are rotating in all solid phases, (b) the CH_3NH_3 ion executes some librational motion in phase II and (c) the methylammonium ions undergo translational diffusion in phase I.

In this paper we present temperature dependent measurements of the proton second moment, M_2, and proton spin-lattice relaxation times, T_1, $T_{1\varrho}$, and T_{1d} in 1 MAP, 1 MA-dP and 1 M-dAP and of deuteron line shape and deuteron Zeeman relaxation T_{1D} in 1 MA-dP and 1 M-dAP in all phases. Analysis of these data yields a rather detailed picture of molecular motions of the cations. By relating these NMR results to the entropy changes associated with the phase transitions as derived from DSC, indirect information about the motions of the ClO_4 anions can be inferred.

2. Experimental

$CH_3NH_3ClO_4$ and $CD_3NH_3ClO_4$ were prepared by neutralization of the free bases with perchloric acid. The salts were recrystalized from isopropyl alcohol and dried over P_2O_5 in a vacuum desicator. $CH_3ND_3ClO_4$ was obtained from fully protonated material by exchange with heavy water. The purity of the samples was checked by elementary analysis. Samples of powdered salts were sealed under vacuum in glass tubes after evacuation for several hours.

The phase transitions were detected by DSC (Perkin-Elmer-2C) with a heating rate of 5 K/min. The temperature of the transitions was determined at the maximum of the thermogram.

The enthalpy of transition, per weight of the material in the sample pan, was derived from the area of the transition peak.

Proton broad-line measurements were carried out on a home-made marginal oscillator spectrometer operating at 28 MHz. Second moments were calculated by numerical integration from the first derivative of the absorption line and corrected for finite modulation amplitude. Pulsed proton NMR experiments were performed with a home-made pulse spectrometer operating at 25 MHz [8]. Spin-lattice relaxation times in the laboratory frame, T_1, were measured using the $90° - t - 90°$ pulse sequence. Spin-lattice relaxation times in the rotating frame, $T_{1\varrho}$, were determined by spin-locking the magnetization in a rotating frame [9]. Spin-lattice dipolar relaxation times, T_{1d}, were measured using the Jeener-Broekaert pulse sequence [10].

The deuteron NMR experiments were performed at a frequency of 55.2 MHz using a modified Bruker pulse spectrometer. The quadrupole split deuteron NMR spectra were obtained using a phase alternating solid-echo sequence $90^\circ_x - \tau_1 - 90^\circ_y$ [11, 12], where the phase of the first pulse was alternated between 0 and 180° and the echo signal alternately added and substracted to the computer memory to form the accumulated echo signal. About 10^3 K scans were averaged and the echo signal was Fourier transformed from its maximum to obtain the undistorted spectrum. The deuteron spin-lattice relaxation times, T_{1D}, were determined by observing the recovery of the magnetization following the application of a saturation sequence of 90° pulses. The quadrupole echo sequence was applied at various intervals t following the initial saturation pulse sequence. The temperature of the sample was varied by a conventional gas flow system heating the samples from low to high temperature phase with an accuracy of 1 K.

3. Results

DSC studies show that 1 MAP, 1 MA-dP and 1 M-dAP udergo three different phase transitions, the associated transition temperatures and the enthalpy changes are presented in Table 1. The transition from the low-temperature phase III to the intermediate phase II takes place at almost identical temperatures for all three salts while the transition from the intermediate phase II to the high-temperature phase I for 1 MAP and 1 M-dAP occurs at an appreciably higher temperature than that for 1 MA-dP. The same observations refer to the

Table 1. Transition temperatures from the low-temperature phase III to the intermediate phase II and from the intermediate phase II to the high-temperature phase I and the enthalpies and entropies associated with these phase transitions for $CH_3NH_3ClO_4$, $CD_3NH_3ClO_4$ and $CH_3ND_3ClO_4$.

Compound	Transition III–II			Transition II–I		
	T (K)	Enthalpy (kJ/mol)	Entropy (J/mol K)	T (K)	Enthalpy (kJ/mol)	Entropy (J/mol K)
$CH_3NH_3ClO_4$	320.6	6.71	20.9	451.1	7.64	16.9
$CD_3NH_3ClO_4$	322.6	6.49	20.1	451.3	7.44	16.5
$CH_3ND_3ClO_4$	319.7	3.82	11.9	437.0	5.48	12.5

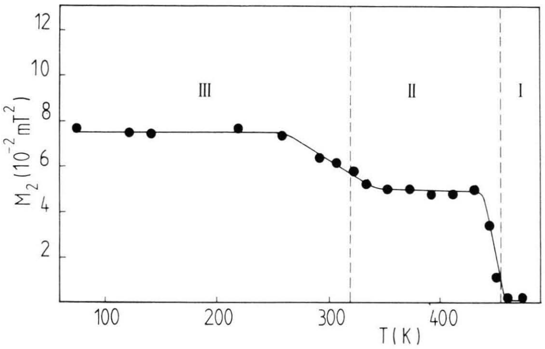

Fig. 1. Proton second moments versus temperature for $CH_3NH_3ClO_4$.

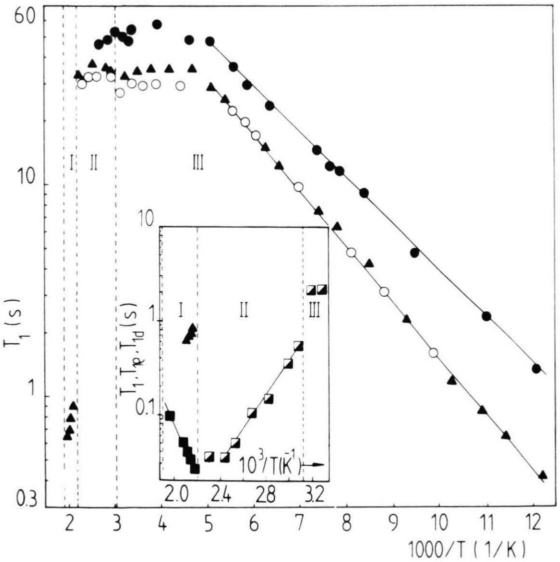

Fig. 2. Temperature dependence of proton T_1 for $CH_3NH_3ClO_4$ (▲), $CH_3ND_3ClO_4$ (●) and $CD_3NH_3ClO_4$ (○), T_{1d} for $CH_3NH_3ClO_4$ (◪) and $T_{1\varrho}$ for $CH_3NH_3ClO_4$ (■).

enthalpy changes associated with the phase transitions. Since all the transitions, due to the temperature hystereses observed, are assumed to be of first order, the associated entropy changes are given by the ratios of the enthalpies of transitions to the measured transition temperatures and are listed in Table 1. All of them were melting below 530 K.

The temperature dependence of the proton second moment M_2 for 1 MAP, plotted in Fig. 1, is found to have two plateau values of 0.076 and 0.050 mT^2. Above 440 K a further line narrowing appears, resulting finally in a liquid-like line shape in phase I. The temperature dependences of the proton spin-lattice relaxation times T_1, $T_{1\varrho}$ and T_{1d} for 1 MAP, 1 MA-dP and 1 M-dAP are plotted simultaneously in Fig. 2 in order to show the differences between the isotopic species. We find that in phase III the T_1's for all compounds increase with increasing temperature having almost the same values for 1 MAP and 1 M-dAP and different ones for 1 MA-dP. On approaching phase II, the T_1 values reach the broad maxima – differing somewhat in absolute value for all three salts – which are not, however, substantially affected by the phase transition III–II. In phase II for 1 MAP we observe a decrease of the dipolar spin-lattice relaxation time T_{1d} with increasing temperature, however we have not reached a minimum in the temperature range preceding the transition III–II. At the II–I phase transitions we observe discontinuities of the T_1 relaxations for all compounds (shown for 1 MAP in Fig. 2). The $T_{1\varrho}$ relaxation times measured at a spin-locking field B_1 of 2.2 mT in phase I increase and the T_1's decrease on raising the temperature, however we were not able to reach a minimum of $T_{1\varrho}$ nor of T_1.

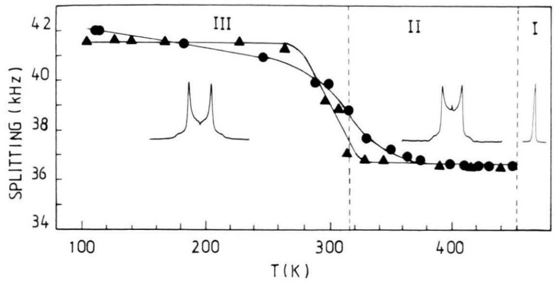

Fig. 3. Observed deuteron NMR spectra in $CH_3ND_3ClO_4$ and $CD_3NH_3ClO_4$ in phases III, II and I, and temperature dependence of the splitting measured between the singularities of the spectra for $CH_3ND_3ClO_4$ (●) and $CD_3NH_3ClO_4$ (▲).

The temperature dependence of the deuteron line-shape for 1 MA-dP and 1 M-dAP is shown in Figure 3. The line-shape for both compounds in phases III and II is the reduced Pake spectrum of the spin 1 the width of which, measured between the singularities, amounts to 42 and 41.6 kHz for 1 MA-dP and 1 M-dAP, respectively. On approaching phase II the splitting for both salts decreases and merges into one value of 36.5 kHz in phase II. The transition to phase I is reflected by a dramatic change of the line-shape resulting in a liquid-like isotropic line.

4. Analysis and Discussion

4.1. NMR line-shapes

From the NMR line-shapes structural as well as dynamical information can be obtained. Deuteron NMR spectra contain specific information about hydrogen bonds and rotational motions of ND_3 and CD_3 groups. The conclusions obtained from deuteron NMR ease the analysis of the proton second moments to give information about the motion of CH_3 and NH_3 groups.

4.1.1. Deuteron NMR

The observed low temperature splittings between the singularities of 42.0 and 41.6 kHz for 1 MA-dP and 1 M-dAP, respectively, are well below the value of about 130 kHz, typically observed for the rigid ND_3 and CD_3 groups [13]. Therefore we infer that motions rapid enough to give the reduced Pake spectrum are already present at the lowest temperature attained in this work. It is known that hindered rotational motions of ND_3 or CD_3 groups about their threefold axes along the N–C bond reduce the effective electric field gradient (efg) experienced by the deuteron by

$$\Delta\nu_m/\Delta\nu_r = \tfrac{1}{2}\,(3\cos^2\vartheta - 1), \qquad (1)$$

Where the $\Delta\nu_m$ abd $\Delta\nu_r$ refer to the splittings of mobile and rigid units, respectively, and ϑ is the angle between the N–D or C–D bond and the rotation axis.

Inserting the observed values of 42.0 and 41.6 kHz and the angle $\vartheta = 70.5°$ [14] into (1) we would expect the splittings of rigid ND_3 and CD_3 groups as 126 and 125 kHz, respectively, in the low-temperature range not covered by our experiment. It is worth noticing that the expected quadrupole coupling constant (QCC) of 168 kHz for the ND_3 group is in agreement with the postulated existence of hydrogen bonds N–H ... O in 1 MAP [4]. The correlation between hydrogen bond length and QCC value for hydrogen bonded systems N–D ... O is given by [4]

$$\mathrm{QCC} = 253 - 0.572\,R^{-3}\ \text{(kHz)}, \qquad (2)$$

where R is the D ... O distance in nm. Inserting the value of QCC = 168 kHz we find $R = 0.188$ nm, in good agreement with the D ... O distances for linear hydrogen bonds estimated from [4].

The decrease of the splitting of the Pake spectra observed with rising temperature (Fig. 3) is assumed to indicate a new motion of the central C–N bond about a rotational axis of threefold or higher symmetry, C_3', which forms a small angle with the C–N bond. The observed plateau of $\Delta\nu$ in phase II indicates that the frequency of this motion is much higher than the spectral width. Using again (1), the angle α between the C–N bond (C_3 axes) and the C_3' axis of rotation can be estimated to be 18 degrees. Thus the phase transition III–II triggers a new degree of restricted motional freedom of the cation. This motional model is consistent with that derived from proton second moment studies (Section 4.1.2).

A dramatic change of the line-shape in phase I evidences that the cations perform a fast quasi-isotropic motion in this phase. This, and the extreme narrowing of the proton solid spectrum proves that the cations undergo also translational motion.

4.1.2. Second moment of proton NMR

In order to identify the types of reorientation responsible for the temperature variation of the proton second moment we have to compare the values observed of second moment plateaus with those calculated for various possible motional modes. The total rigid lattice value of the second moment, being the sum of intra- and intermolecular parts, cannot be calculated precisely due to lack of structural information concerning the proton positions for 1 MAP. However, we can estimate the second moments in our case using those calculated for CH_3NH_3Cl [15]. The proton intramolecular second moment for threefold reorientation of CH_3 and NH_3 groups about the C–N axis, C_3, considering its rigid value as 0.308 mT^2, ranges from 0.0745 to 0.0817 mT^2, covering thus the plateau value of 0.076 mT^2 observed for 1 MAP. The decrease in M_2 from 0.076 to 0.050 mT^2 can be interpreted as a result of a new motion the frequency of which is high enough to narrow the resonance line. The relatively small decrease in M_2 – in accord with the deuteron line-shape results – allows us to assume again that it arises from a motion of the C–N bond about a threefold – or higher – symmetry axis C_3' forming a small angle with this bond. The reduced value of the intramolecular second moment is then given by

$$M_2(C_3') = M_2(C_3)\,\frac{(1-3\cos^2\alpha)^2}{4}\,, \tag{3}$$

where $M_2(C_3')$ and $M_2(C_3)$ refer to the second moments for C_3' and C_3 motions, respectively. Assuming $\alpha = 18°$ as from the deuteron spectra we find $M_2(C_3')$ – making the reasonable assumption concerning the intermolecular interactions [16] – as 0.053 mT^2, which agrees fairly well with the value observed experimentally.

A sudden narrowing of the resonance line with a second moment close to zero on going to the phase I is assigned to self-diffusion of the cations in the cubic crystal of 1 MAP. The appearance of this motion in polyatomic ionic solids is exceptional and has so far been observed only in $(CH_3)_3NHClO_4$ [5], $(CH_3)_2NH_2ClO_4$ [6], NH_4NO_3 [17] and $CH_3NH_3NO_3$ [18].

4.2. *Relaxation studies*

The deuteron and proton NMR line-shapes considered so far yield information about the type of molecular motions occurring in the various phases. Additional information about the timescale, and in particular about the activation energies of different motions can be determined by deuteron and proton relaxation studies. Moreover, by studies of selectively deuterated monomethylammonium perchlorates we will be able to find whether the motions of the CH_3 and NH_3 groups are independent of each other or not.

4.2.1. Deuteron relaxation

The spin-lattice relaxation times T_{1D} in the phases III and II for 1 M-dAP and 1 MA-dP are assumed, following our deuteron and proton line-shape studies, to be controlled by the threefold C_3 reorientation of the CD_3 and ND_3 groups about the C–N axis and the reorientations of the CD_3NH_3 and CH_3ND_3 ions about a threefold – or higher – symmetry C_3' axis, presumably lying on a symmetry axis of the unit cell, forming an angle α with the C_3 axis of CD_3 and ND_3 groups. Since the transition III–II does not affect the relaxation times, we assume that the correlation times change continuosly going from phase III to phase II. The spin-lattice relaxation rate for such a model of motion, under the assumption that the relaxation is completely dominated by the quadrupole interaction of the deuteron is expressed as follows [19, 20]

$$\frac{1}{T_{1D}} = \frac{9}{640}\left(\frac{e^2qQ}{\hbar}\right)^2 [A\,g(\omega_0,\tau_c) + B\,g(\omega_0,\tau_{c2}) + C\,g(\omega_0,\tau_{c3})]\,,$$

where $e^2qQ/\hbar$ is the quadrupole coupling constant, τ_c and τ_{c2} are the correlation times for C_3 and C_3' reorientations, respectively, and $\tau_{c3}^{-1} = \tau_c^{-1} + \tau_{c2}^{-1}$. The spectral density function $g(\omega_0, \tau_i)$, where $i = c_1, c_2, c_3$ is expressed as

$$g(\omega_0,\tau_i) = \frac{\tau_i}{1+\omega_0^2\tau_i^2} + \frac{4\tau_i}{1+4\omega_0^2\tau_i^2}\,. \tag{5}$$

The constants A, B and C have the form

$$\begin{aligned} A &= \tfrac{3}{2}\,(\sin^4\alpha\sin^4\vartheta + \sin^2 2\alpha\sin^2 2\vartheta)\,,\\ B &= \sin^2\alpha\,(1+3\cos^2\alpha)\,(3\cos^2\vartheta-1)^2\,, \qquad (6)\\ C &= \tfrac{1}{2}\sin^4\vartheta\,(8-3\sin^4\alpha) + \tfrac{1}{2}\sin^2 2\vartheta\,(8-3\sin^2 2\alpha)\,, \end{aligned}$$

where ϑ is the angle between the N–D or C–D bond and the reorientation axis C_3, and α is the angle between the C_3 and C_3' axes.

Table 2. Activation energies E_A and inverse frequency factors τ_0 for reorientation of the CH_3, CD_3, NH_3 and ND_3 groups about their C_3 axes, reorientation of the cations about the C_3' axis, and self-diffusion (SD) of the cations in $CH_3NH_3ClO_4$, $CD_3NH_3ClO_4$ and $CH_3ND_3ClO_4$.

Compound	Motion	Phase	E_A (kJ/mol)	τ_0 (s)
$CH_3ND_3ClO_4$	CH_3 (C_3)	III	4.21	4.06×10^{-14}
$CD_3CH_3ClO_4$	CD_3 (C_3)	III	4.27	4.50×10^{-14}
$CD_3NH_3ClO_4$	NH_3 (C_3)	III	5.11	2.75×10^{-14}
$CH_3ND_3ClO_4$	ND_3 (C_3)	III	3.56	9.50×10^{-14}
$CH_3NH_3ClO_4$	CH_3 (C_3)	III	4.23	4.06×10^{-14}
$CH_3NH_3ClO_4$	NH_3 (C_3)	III	5.36	3.20×10^{-14}
$CH_3NH_3ClO_4$	$CH_3NH_3^+$ (C_3')	II	36.9	–
$CD_3NH_3ClO_4$	$CD_3NH_3^+$ (C_3')	II	36.9	8×10^{-12}
$CH_3ND_3ClO_4$	$CH_3ND_3^+$ (C_3')	II	36.9	8×10^{-12}
$CH_3NH_3ClO_4$	$CH_3NH_3^+$ (SD)	I	49.0	1.5×10^{-13}

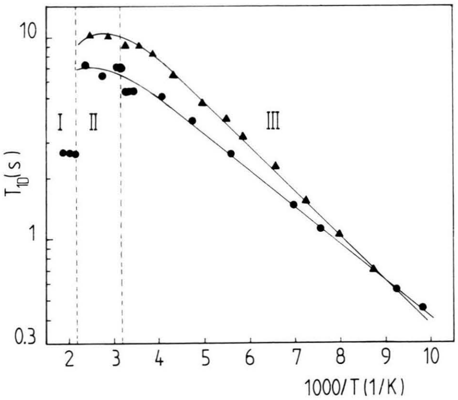

Fig. 4. Temperature dependence of deuteron T_{1D} for $CH_3ND_3ClO_4$(●) and $CD_3NH_3ClO_4$ (▲).

In order to fit our T_{1D} data with (4) we made the usual assumption that the motions responsible for relaxation are thermally activated, i.e. that

$$\tau_{ci} = \tau_{0i} \exp(E_{Ai}/RT). \tag{7}$$

Taking $\vartheta = 70.5°$, $\alpha = 18°$, QCC = 166 kHz, and the activation energy for the C_3' motion derived from the slope of proton T_{1d} (next section) as 36.9 kJ/mol, we found the best fits shown by the solid lines in Fig. 4 for the activation parameters listed in Table 2.

4.2.2. Proton relaxation

The proton spin-lattice relaxation times of 1 MAP, 1 MA-dP and 1 M-dAP in the phases III and II likewise are believed to be controlled by the C_3 reorientation of the CH_3 and NH_3 groups about the C–N axis and by reorientation of the whole ion about the C_3' axis. Under the assumption that the relaxation is completely dominated by intramolecular proton dipole-dipole interaction, the spin-lattice relaxation rate of the CH_3 group in 1 MA-dP, or of the NH_3 group in 1 M-dAP is expressed by [21]

$$\begin{aligned}\frac{1}{T_1} = \frac{9}{80}\frac{\gamma^4 \hbar^2}{r^6}\,[\tfrac{3}{2}\sin^4\alpha\, g(\omega_0, \tau_c) \\ + \sin^2\alpha\,(1+3\cos^2\alpha)\, g(\omega_0, \tau_{c2}) \\ + \tfrac{1}{2}\,(8-3\sin^2\alpha)\, g(\omega_0, \tau_{c3})],\end{aligned} \tag{8}$$

where r is the interproton distance within the CH_3 or NH_3 group, and the other symbols have the same meaning as in the expressions for the deuteron relaxation. Taking r values of 0.179 and 0.170 nm for CH_3 and NH_3 groups, respectively [15], and assuming that the motions are thermally activated according to (7), we have determined the activation parameters, listed in Table 2, for the C_3 motion of the CH_3 group in 1 MA-dP and the NH_3 group in 1 M-dAP. However, the broad maximum of T_1 observed at higher temperatures is somewhat lower than predicted by these parameters. Since the phase transition III–II does not affect the proton relaxation substantially, we believe that this transition is mainly due to the change of motional behaviour of the ClO_4^- groups. Then a new relaxational mechanism involving proton-oxygen dipolar interaction can not be ruled out. Although this contribution is very weak it can be competitive with the intramolecular relaxation at high temperatures. The coincidence of the proton T_1 data for fully protonated 1 MAP with those for the selectively deuterated 1 M-dAP may be somewhat surprising, since one would expect these values to differ from each other. However, if one takes into account that the phase transitions III–II of both compounds are shifted by 2 degrees (Table 1), then such a coincidence is possible. Knowing the motional behaviour of the CH_3 and NH_3 groups in selectively deuterated methylammonium perchlorates we can analyze the relaxation of the fully protonated compound. The spin-lattice relaxation rate for 1 MAP is assumed to be the sum of the two independent contributions arising from the C_3 and C_3' reorientations of CH_3 and of NH_3 groups:

$$\frac{1}{T_1} = \frac{1}{2}\frac{1}{T_1^{(CH_3)}} + \frac{1}{2}\frac{1}{T_1^{(NH_3)}}, \tag{9}$$

where $1/T_1^{(CH_3)}$ and $1/T_1^{(NH_3)}$ are expressed by (8). Taking the activation parameters for the C_3' motion the selectively deuterated compounds and for the CH_3 motion those determined in 1 MA-dP (Table 2) we are able to obtain the motional parameters of the NH_3 group in 1 MAP treating them as adjustable parameters. With these assumptions we found the best fit to our relaxation data for the activation parameters listed in Table 2. We failed again to find a reasonable fit to the observed maximum of T_1 with the motional parameters of the C_3' motion presumably for the same reasons as discussed for the proton relaxation in 1 M-dAP and 1 MA-dP. It is worth noting that the activation energy of the NH_3 group differs only by 5% from that in 1 M-dAP, and that the low-temperature adjustable solid line would be shifted by 1.8° with respect to the experimental data only of one took for the fitting procedure the value determined for the NH_3 group in 1 M-dAP. This difference agrees very well with the observed difference between the transition temperatures III–II for 1 MAP and 1 M-dAP (Table 1).

Neither proton nor deuteron spin-lattice relaxation times T_1 are sensitive for the phase transition III–II, however the slow motion of the C–N bond about the C_3' axis derived from the proton and deuteron line shape analysis is evidenced by short proton dipolar spin-lattice relaxation times T_{1d} in phase II, the slope of which leads to an activation energy of 36.9 kJ/mol. Since the correlation times in this temperature range are believed to be of the order of T_2 for the rigid lattice the evaluation of a preexponential factor should be performed using the strong collision approach [22], which requires in turn a knowledge of structural data in this phase not available at present.

Extreme narrowing of the proton and deuteron line-shapes, the flat behaviour of the deuteron T_{1D}, the decrease in proton T_1 and the increase in proton $T_{1\varrho}$ with temperature indicate that translational motion (self-diffusion) takes place in phase I. Such a motion completely averages the intramolecular proton interaction and also averages the residual intermolecular interaction leading thus to a proton linewidth close to that associated with the liquid state. A clear evidence for isotropic rotational motion comes from the narrow deuteron line (Fig. 3), whith a width of 4 kHz only. A flat behaviour of T_{1D} with temperature manifests that the energy barrier of this motion is lower than that in phases III and II. The interpretation of spin relaxation studies of translational diffusion is usually based on Torrey's "lattice diffusion" random-walk model [23] assuming that the molecules perform jumps of equal length to nearest-neighbouring positions. For this model in the case of a cubic lattice the frequency-dependent decrease in T_1 and the frequency-independent increase in $T_{1\varrho}$ can be expressed as [23, 24]

$$\frac{1}{T_1} = 2.24\frac{M_2\gamma^2}{\omega_0^2\tau_D}, \tag{10}$$

$$\frac{1}{T_{1\varrho}} = 0.955\,M_2\gamma^2\tau_D, \tag{11}$$

where τ_D is the correlation time for the diffusion assumed to be a thermally activated process according to (7) and M_2 is the second moment value prior to the diffusion process. With these two equations, taking the activation energy derived from the slope of $T_{1\varrho}$ as 49.0 kJ/mol, we found the two adjustable parameters M_2 and τ_{0D} as 0.0088 mT^2 and 1.5×10^{-13} s, respectively. Although we have not observed a plateau of $M_2 = 0.0088$ mT^2 prior to diffusional narrowing because of the phase transition II–I, this value can be calculated from the known lattice parameter for an endospherical reorientational motion using the following expression for the dipolar interaction between the nuclei in a polycrystalline sample of 1 MAP [25]:

$$M_2 = \tfrac{3}{5}N\gamma^2\hbar^2 I(I+1)\sum_i r_{ij}^{-6}. \tag{12}$$

Since we have rapid endospherical reorientation, it is assumed that all N nuclei in a given molecule can be considered to be located at the appropriate molecule's lattice site. In this situation the lattice sum $\sum r_{ij}^{-6}$ becomes $8.5a^{-6}$ for a simple cubic lattice, where a is the lattice constant. With $a = 0.518$ nm [3] and $N = 6$ we calculate $M_2 = 0.0094$ mT^2, which compares well with that found in experiment. Thus we conclude that the model of random walk diffusion assumed describes the self-diffusion of the methylammonium ions in 1 MAP correctly.

4.3. Differential scanning calorimetry

The entropy changes associated with the observed phase transitions, listed in Table 1, indicate that there is a strong isotope effect for 1 MA-dP. The total change in entropy is the sum of electronic, vibrational, rotational and configurational contributions [1]. In our case, however, only vibrational and configurational contributions are believed to account for the entropy changes. The vibrational part is determined by the vibrational spectrum of the sample, which in the case of the ND_3 groups involved in N−D ... O hydrogen bonds is quite different from that of 1 MAP or 1 M-dAP with NH_3 hydrogen-bonded to ClO_4 groups. This is believed to be a reason for the different values of the enthalpies observed and consequently the entropy changes associated with the 1 MAP and 1 M-dAp. the smaller value of the enthalpy change for 1 MA-dP than for 1 MAP and 1 M-dAP is understandable since N−D ... O hydrogen bonds are weaker than N−H ... O. By subtracting from the observed value the vibrational term, the configurational entropy is obtained. It is believed to account for the orientational disorder of the ions. Since our NMR studies show no abrupt change of the motional behaviour of the cations on going from phase III to phase II, we conclude that the perchlorate ions are those which gained orientational freedom at this phase transition. The disordering process is described with a fair accuracy as $R \ln(n)$ [1], where n is an integer or simple fraction giving the ratio of the number of orientational states in the higher – and lower – temperature phase, respectively. For a number of transitions in salts typical values of n are: $2 \leqq n \leqq 4$. It is worth noticing that – neglecting the vibrational contribution in 1 MA-dP for the moment – the entropy change of the III−II phase transition corresponds to $n = 4$, which is a reasonable number. On the other hand, for 1 MAP and 1 M-dAP the same assumption would give $n = 12$. This strongly suggests that in the compounds involving N−H ... O hydrogen bonds the vibrational part gives a significant contribution to the entropy change at the III−II phase transition. Our recent high-field Cl-35 NMR measurements for these compounds provide a convincing evidence for the interrelation between the occurrence of the phase transition III−II and a change of the molecular dynamics of the ClO_4 groups [26]. A major change of ClO_4 motion occurs just at the phase transition III−II, whereas a much smaller change in mobility is observed at the phase transition II−I. Therefore, since the methylammonium ions perform an anisotropic motion in phase II and an isotropic motion in phase I, we associate the observed entropy changes from phase II to phase I with a gain of new motional degrees of freedom by the cations.

5. Concluding Comments

It is evident from our measurements that the phase transitions III−II and II−I in 1 MAP, 1 M-dAP and 1 MA-dP are triggered by the motions of the anions and cations, respectively. The NMR studies clearly show that the CH_3 and NH_3 groups in phase III are independently overcoming different energy barriers (Table 2). The smaller energy barrier for the C_3 motion of the ND_3 group as compared to that of the NH_3 group indicates that the latter forms a stronger hydrogen-bond to ClO_4^- than the former. The activation energies for the CH_3 and CD_3 groups are, however, almost the same, showing that these groups are not involved in hydrogen bonds, as expected. Since the selective deuteration of the methyl group does not change its activation energy, it is believed that the origin of the reorientational barrier for the C_3 motion of the methyl groups is rather of inter- than intramolecular origin. We would like to mention that the proton T_1 and T_2 measurements of 1 MAP by Ishida et al. [18] yield an activation energy for the C_3 motion in agreement with what we find [7], however, the activation energy for translational motion determined from T_2 data is smaller by a factor of 1.7 than derived from our $T_{1\varrho}$ measurements.

Our proton and deuteron NMR data can be compared with those for the analogous tri- and dimethylammonium salts [5, 6], which undergo two solid-solid phase transitions as well. In the low-temperature range of phase III, apart from the methyl group reorientation, the cations do not undergo any motion. The transition to phase II is associated with some ionic motion, and in the case of the dimethylammonium perchlorate there is a substantial change of the molecular motion of the perchlorate ions. The transition to phase I is manifested by isotropic reorientation of the ions along with self-diffusion. Phase I, resembling by its nature molecular plastic crystals [1], seems to be a common feature of the ammonium solids with highly mobile ClO_4^- groups [5–7, 18], NO_3^- groups [17, 18] and BF_4^- groups (our unpublished data). For tri-, di- and monomethylammonium perchlorates we observe that the activation energy for self-difusion increases with II–I transition temperatures.

In summary, our measurements enabled us to identify the motions occurring in the respective phases. In the low-temperature range of phase III the CH_3 and NH_3 groups undergo reorientation about the threefold symmetry axis with different frequencies overcomming different energy barriers. Also in this temperature range the quadrupole coupling constant indicates that the monomethylammonium and perchlorate ions are hydrogen-bonded systems with the average D ... O distance of 0.188 nm. On approaching phase II we observe the onset of the motion of the monomethylammonium ion about a symmetry axis, inclined at an angle of 18° to the C_3 axis. This motion is fully activated in phase II. The analysis of the entropy changes associated with the III–II transitions indicates that the ClO_4^- ions have a large motional freedom in phase II, presumably because of breaking or weakening of N–H ... O hydrogen bonds. In phase I the monomethylammonium ions undergo isotropic motion along with translational diffusion between different sites of the primitive cubic unit cell.

Acknowledgements

The fellowship to S. Jurga from the Alexander von Humboldt Foundation is gratefully acknowledged. We wish to thank R. Ebelhaeuser for preparing the selectively deuterated $CD_3NH_3ClO_4$ compound.

[1] N. G. Parsonage and L. A. K. Staveley, Disorder in Crystals, Clarendon Press, Oxford 1978.
[2] M. Molitor, W. Müller-Warmuth, H. W. Spiess, and R. Schöllhorn, Z. Naturforsch. **38a**, 237 (1982).
[3] M. Stammler, R. Bruenner, W. Schmidt, and D. Orcutt, Adv. X-Ray Anal. **9**, 170 (1966).
[4] P. F. Zanazzi, Acta Cryst. **B 24**, 499 (1968).
[5] S. Jurga, Phys. Stat. Solidi (a) **81**, 77 (1984).
[6] S. Jurga and H. W. Spiess, Ber. Bunsenges. Phys. Chem. **89** (1985).
[7] S. Jurga, K. Jurga, and Z. Pajak, Bull. Magn. Resonance **2**, 245 (1981).
[8] K. Jurga, J. Phys. E **14**, 555 (1981).
[9] D. C. Look and I. J. Lowe, J. Chem. Phys. **44**, 2995 (1966).
[10] J. Jeener and P. Broekaert, Phys. Rev. **157**, 232 (1967).
[11] R. Hentschel and H. W. Spiess, J. Magn. Resonance **35**, 157 (1979).
[12] H. W. Spiess, J. Chem. Phys. **72**, 6755 (1980).
[13] R. G. Barnes, in: Adv. in Nuclear Quadrupole Resonance, Vol. 1, p. 335, Ed. J. A. S. Smith, Heyden, London 1974.
[14] M. J. Hunt and A. L. Mackay, J. Magn. Reson. **15**, 402 (1974).
[15] E. R. Andrew and C. P. Canepa, J. Magn. Reson. **7**, 429 (1972).
[16] G. W. Smith, J. Chem. Phys. **42**, 4229 (1965).
[17] M. T. Riggin, R. R. Knispel, and M. M. Pintar, J. Chem. Phys. **56**, 2911 (1972).
[18] H. Ishida, R. Ikeda, and D. Nakamura, Chem. Letters **1982**, 1943.
[19] H. W. Spiess, in: NMR, Basic Principles and Progress, ed. by P. Diehl, E. Fluck, and R. Kosfeld, Vol. 15, p. 55, Springer-Verlag, Berlin 1978.
[20] S. Jurga, K. Jurga, and Z. Pajak, J. Magn. Reson. **50**, 175 (1982).
[21] M. B. Dunn and C. A. McDowell, Mol. Phys. **24**, 969 (1972).
[22] D. Ailion and C. P. Slichter, Phys. Rev. **137A**, 235 (1965).
[23] H. C. Torrey, Phys. Rev. **92**, 962 (1953); **96**, 690 (1954).
[24] N. Boden, J. Cohen, and R. T. Squires, Mol. Phys. **31**, 1813 (1976).
[25] A. Abragam, The Principles of Nuclear Magnetism, Oxford University Press, Oxford 1961.
[26] S. Jurga, F. Fujara, and H. W. Spiess, to be published.